Design of an Extended Kalman Filter for UAV Localization

Conference Paper · March 2007

DOI: 10.1109/IDC.2007.374554 · Source: IEEE Xplore

3 authors, including:

Guoqiang Mao
Xidian University
298 PUBLICATIONS **7,434** CITATIONS
SEE PROFILE

Samuel Picton Drake
University of Adelaide
39 PUBLICATIONS **527** CITATIONS
SEE PROFILE

Design of an Extended Kalman Filter for UAV Localization

Guoqiang Mao*§, Sam Drake ‡ and Brian D. O. Anderson †¶
*School of Electrical and Information Engineering, the University of Sydney.
† Research School of Information Sciences and Engineering, Australian National University
‡ Defence Science and Technology Organization (DSTO), Australia
§ National ICT Australia Limited[1], Sydney, Australia
¶National ICT Australia Limited, Canberra, Australia

Abstract

Unmanned aerial vehicles (UAVs) are increasingly used in military and scientific research. Some miniaturized UAVs rely entirely on the global positioning system (GPS) for navigation. GPS is vulnerable to accidental or deliberate interference that can cause it to fail. It is not unusual, even in a benign environment, for a GPS outage to occur for periods of seconds to minutes. For UAVs relying solely on GPS for navigation such an event can be catastrophic. This paper proposes an extended Kalman filter approach to estimate the location of a UAV when its GPS connection is lost, using inter-UAV distance measurements. The results from a recent trial conducted by DSTO in Australia with three UAVs are presented. It is shown that the location of a manoeuvering UAV that has lost the GPS signal can be determined to an accuracy of within $40m$ *of its true location simply by measuring the range to two other UAVs at known location, where the range measurement error has a zero mean and a standard deviation of* $10m$.

1. Introduction

Unmanned aerial vehicles (UAVs) are increasingly used in military and scientific research. UAVs rely on accurate location information for a variety of purposes including navigation, motion planning and control, and mission completion. Most UAVs obtain their location from the global positioning system (GPS), inertial navigation system, or a combination of both [1]. Because of constraints on cost and payload size, there is a significant number of UAVs equipped with GPS equipment only. For example the mini-UAVs used by DSTO are the Aerosonode UAVs which navigate with a GPS receiver and altimator. The GPS signal is easily affected by external interference, noise or receiving equipment failure/malfunction. For those UAVs equipped with GPS only, it has been observed in the real experiments that some of them may temporarily lose their GPS connection for a quite long time. In such a case, those UAVs losing their GPS connection have to be brought down and their mission will be aborted due to safety concerns. Consequently, to avoid this outcome it is desirable to design an approach which can estimate the location of those UAVs which temporarily lose their GPS connection.

In this paper, we propose using range measurements in conjunction with an extended Kalman filter (EKF) to estimate the location of those UAVs temporarily losing their GPS connection. Specifically, we consider a group of UAVs with possibly different functionalities cooperating with each other to complete a mission, e.g., reconnaissance, video imaging, etc. These UAVs are able to measure distance between each other. During the flight, some UAVs may temporarily lose their GPS connection. However at any time, there are at least two UAVs, which are able to maintain their GPS connection. A UAV without GPS connection uses the proposed EKF, whose observations are the distance measurements to UAV with GPS navigation, to estimate its own location.

The rest of the paper is organized as follows. In Section 2 we discuss the general principle of localizing UAVs with range measurements. Section 3 introduces the design of the EKF. Section 4 introduces the UAV trajectories obtained from a recent trial conducted by DSTO in Australia with three UAVs. These data are used in the later simulation. Section 5 presents the simulation results. Finally, conclusions are given in Section 6.

2. Localizing with Range Measurements

Generally speaking, in 2D scenarios range measurements to three non-collinear nodes with known location (i.e., UAVs with known location) are required to uniquely determine the location of a node. When range measurements to only two nodes with known location are available, a situation referred to as flip ambiguity may occur. This is illustrated in Fig. 1.

For the specific problem considered in this paper, i.e., estimating the location of a UAV *temporarily* losing its GPS connection, the location of the UAV before it loses its GPS connection may be usable to resolve the flip ambiguity shown in Fig. 1. That is, the UAV location before GPS outage may help to determine on which side of the two known nodes (i.e., two UAVs with known location) the UAV is located. Therefore range measurements to two UAVs with known location may be sufficient to uniquely determine the location of a UAV temporarily losing its GPS connection. However it should

[1]National ICT Australia is funded by the Australian Governments Department of Communications, Information Technology and the Arts and the Australian Research Council through the *Backing Australias Ability initiative* and the ICT Centre of Excellence Program.

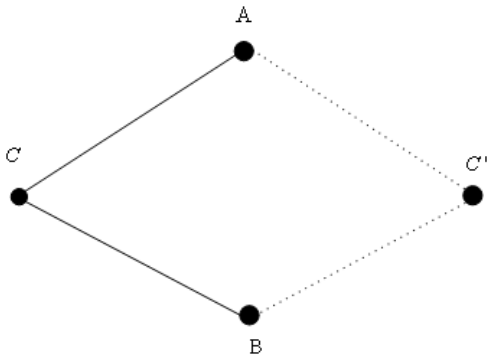

Fig. 1: An illustration of the flip ambiguity in 2D. Using range measurements to nodes A and B at known location only, node C is unable to determine whether its true location is at C or C'.

be noted that using range measurements to only two UAVs with known location, the flip ambiguity problem may still occur in some special cases. This is shown in Fig. 2. When this happens, additional information such as the maximum angular velocity of the UAV has to be considered to resolve the ambiguity.

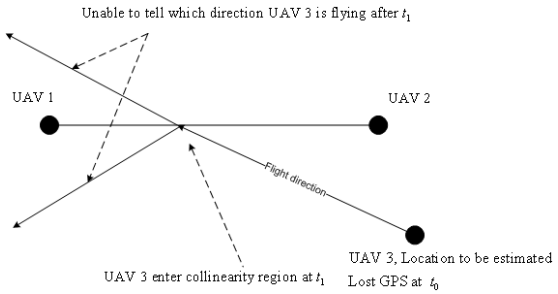

Fig. 2: Using range measurements to only two UAVs with known location, the flip ambiguity problem may still occur in some special cases. Specifically, when UAV 3 crosses the line of UAV 1 and UAV 2 (with known location) after t_1, UAV 3 is unable to uniquely determine its location using range measurements to UAV 1 and 2 only.

In summary, depending on the movement pattern of the UAV and the geometric relationship between the UAV temporarily losing its GPS connection and the UAVs with GPS connection, in 2D range measurements to two UAVs with GPS connection may be sufficient to estimate the location of the UAV temporarily losing its GPS connection.

3. Design of the Extended Kalman Filter

It is assumed that the movement of the UAV in the vertical plane and in the horizontal plane can be decoupled [2]. This paper considers the movement of UAV in the horizontal plane only, i.e., it considers a 2D localization problem. This assumption is widely used to simplify the modeling of aircraft dynamics [2]. It is further justified by the fact that for the considered applications, the UAVs stay at approximately the same altitude.

The dynamic model of a UAV is given by the following continuous-time equations:

$$\dot{x}(t) = v(t)\cos\eta(t) \quad (1)$$
$$\dot{y}(t) = v(t)\sin\eta(t) \quad (2)$$
$$\dot{\eta}(t) = \omega(t) \quad (3)$$
$$\dot{\omega}(t) = \varepsilon_\omega(t) \quad (4)$$
$$\dot{v}(t) = \varepsilon_v(t) \quad (5)$$

where at time t the state variables $\{x(t), y(t)\}$ are the coordinates of the UAV in the horizontal plane, $\eta(t)$ is the heading of the UAV, $\omega(t)$ is the angular speed of the UAV (i.e., the rate of change of the UAV heading measured in radians per second) and $v(t)$ is the ground speed of the UAV, i.e., a scalar. $\varepsilon_\omega(\cdot)$ and $\varepsilon_v(\cdot)$ are assumed to be stationary, Gaussian, zero mean white noise processes, mutually independent, with known covariances $E[\varepsilon_\omega(t)\varepsilon_\omega(s)]$ and $E[\varepsilon_v(t)\varepsilon_v(s)]$ given by $Q_\omega\delta(t-s)$ and $Q_v\delta(t-s)$ respectively. δ is the Kronecker delta function. They are used to model the acceleration of the UAV speed caused by wind and control maneuver, etc. The values of Q_ω and Q_v are derived from the maximum angular speed of the UAV and an empirical observation of the typical variations in the linear speed of the UAV respectively.

A discrete-time equation set corresponding to Eq. 1 through Eq. 5 will be an approximation because of the nonlinearities in the continuous-time model, and because of the treatment of noise terms. The easiest approximation is that based on an Euler approximation of the equations. This is a well known procedure for deterministic equations, but is also the basis for approximating stochastic equations, and is grounded in Itô calculus [4]. The discrete-time UAV dynamic model is shown in the following.

$$x_{k+1} = x_k + v_k\Delta t_k\cos\eta_k \quad (6)$$
$$y_{k+1} = y_k + v_k\Delta t_k\sin\eta_k \quad (7)$$
$$\eta_{k+1} = \eta_k + \omega_k\Delta t_k \quad (8)$$
$$\omega_{k+1} = \omega_k + \varepsilon_{\omega,k} \quad (9)$$
$$v_{k+1} = v_k + \varepsilon_{v,k} \quad (10)$$

The discrete-time state vector is $\theta_k = [x_k \;\; y_k \;\; \eta_k \;\; \omega_k \;\; v_k]'$. It should approximate the value of the continuous time state vector at the k^{th} distance measurement time, call it t_k. Δt_k is the time interval between the $k+1^{th}$ and k^{th} distance measurement updates. The sequences $\{\varepsilon_{\omega,k}\}$ and $\{\varepsilon_{v,k}\}$ are stationary zero mean white Gaussian sequences of random variables, mutually independent. The covariance of the first of these discrete-time sequence is [6]:

$$E[\varepsilon_{\omega,k}\varepsilon_{\omega,j}] = Q_\omega\Delta t_k\delta_{kj}. \quad (11)$$

Similarly the covariance for the $\{\varepsilon_{v,k}\}$ process is:

$$E[\varepsilon_{v,k}\varepsilon_{v,j}] = Q_v\Delta t_k\delta_{kj}. \quad (12)$$

This means that one can replace Eq. 9 and Eq. 10 by:

$$\omega_{k+1} = \omega_k + \gamma_{\omega,k}\sqrt{\Delta t_k} \quad (13)$$
$$v_{k+1} = v_k + \gamma_{v,k}\sqrt{\Delta t_k}. \quad (14)$$

The sequences $\{\gamma_{\omega,k}\}$ and $\{\gamma_{v,k}\}$ are mutually independent, stationary zero mean white Gaussian sequences of random variables, with covariances Q_ω and Q_v respectively. The advantage of this form is that it displays dependence of discrete-time noise on the interval between successive updates.

In summary, the discrete-time dynamic model of the UAV is taken as in Eq. 15.

$$\theta_{k+1} = \underbrace{\begin{pmatrix} 1 & 0 & 0 & 0 & \Delta t_k \cos\eta_k \\ 0 & 1 & 0 & 0 & \Delta t_k \sin\eta_k \\ 0 & 0 & 1 & \Delta t_k & 0 \\ 0 & 0 & 0 & 1 & 0 \\ 0 & 0 & 0 & 0 & 1 \end{pmatrix}}_{f[\theta_k]} \theta_k + \underbrace{\begin{pmatrix} 0 & 0 \\ 0 & 0 \\ 0 & 0 \\ \sqrt{\Delta t_k} & 0 \\ 0 & \sqrt{\Delta t_k} \end{pmatrix}}_{U_k} \begin{pmatrix} \gamma_{\omega,k} \\ \gamma_{v,k} \end{pmatrix} \quad (15)$$

The measurement equation is:

$$d_k = \underbrace{\sqrt{(x_k - x_0)^2 + (y_k - y_0)^2}}_{h[\theta_k]} + \varepsilon_{d,k} \quad (16)$$

where $\{x_0 \quad y_0\}$ are the coordinates of the UAV from which the k^{th} distance measurement is received and $\{\varepsilon_{d,k}\}$ is a stationary zero mean white Gaussian sequence of random variables, which is used to model the distance measurement error. This sequence is assumed to be independent of $\{\varepsilon_{\omega,k}\}$ and $\{\varepsilon_{v,k}\}$. Note that in real-world application, it is possible that more than one distance measurements is received from multiple UAVs at approximately the same time. In that case the measurement equation can be expanded to include multiple equations like Eq. 16. In this paper, we only consider the more generic situation that at any time, only one distance measurement is received.

Given the non-linear dynamic equation shown in Eq. 15 and the non-linear measurement equation shown in Eq. 16, an estimate of the UAV location $\{x_k \quad y_k\}$ as k varies can be obtained using the extended Kalman filter [5]. Both the dynamic equation and the measurement equation are linearized by keeping the first order term in the Taylor series expansion and ignoring the higher order terms. The procedure of the EKF is shown in the following for completeness.

- State prediction:

$$\hat{\theta}_{k+1|k} = f[\hat{\theta}_{k|k}], \quad (17)$$

  where the function f is defined in Eq. 15.
- Computes the state prediction covariance matrix:

$$P_{k+1|k} = f_x[\hat{\theta}_{k|k}] P_{k|k} f_x'[\hat{\theta}_{k|k}] + U_k Q U_k' \quad (18)$$

  where U_k is defined in Eq. 15 and $f_x[\hat{\theta}_{k|k}]$ is the Jacobian of f evaluated at $\hat{\theta}_{k|k}$. $Q = diag\{Q_\omega \quad Q_v\}$ is the covariance matrix of the error terms $\gamma_{\omega,k}$ and $\gamma_{v,k}$, and is assumed to be known.
- Computes the predicted measurement:

$$\hat{d}_{k+1|k} = h[\hat{\theta}_{k+1|k}], \quad (19)$$

  where the function h is defined in Eq. 16.
- Computes the measurement prediction covariance:

$$S_{k+1} = h_x[\hat{\theta}_{k+1|k}] P_{k+1|k} h_x'[\hat{\theta}_{k+1|k}] + R, \quad (20)$$

  where $h_x[\hat{\theta}_{k+1|k}]$ is the Jacobian of h evaluated at $\hat{\theta}_{k+1|k}$. R is the variance of $\varepsilon_{d,k}$ and is assumed to be a known value.
- Computes the filter gain:

$$W_{k+1} = P_{k+1|k} h_{\hat{\theta}_{k+1|k}} S_{k+1}^{-1} \quad (21)$$

- Updates the state estimate:

$$\hat{\theta}_{k+1|k+1} = \hat{\theta}_{k+1|k} + W_{k+1} \lambda_{k+1} \quad (22)$$

  where λ_{k+1} is called the innovation and defined as:

$$\lambda_{k+1} = d_{k+1} - \hat{d}_{k+1|k} \quad (23)$$

- Updates the state covariance matrix:

$$P_{k+1|k+1} = P_{k+1|k} - W_{k+1} S_{k+1} W_{k+1}' \quad (24)$$

The initial values $\hat{\theta}_{0|0}$, $P_{0|0}$ can be chosen empirically or can be computed from the state of the UAV before GPS outage. The impact of the initial values on the state estimate normally vanishes exponentially fast [5].

4. THE UAV TRAJECTORIES

The proposed approach is validated by simulation using real UAV trajectories. In this section, we give an introduction to the experimental data used in the simulation.

Three UAVs are considered, which are named UAV 1, UAV 2 and UAV 3 respectively. During the flight, the following GPS data were collected: time, geocentric latitude, geocentric longitude, altitude, time of arrival, pulse width, signal frequency and amplitude. The longitude, latitude and height (LLH) coordinates recorded by the UAV are not well suited for navigation and tracking problems because linear motion becomes non-linear in these coordinates. In comparison, a local coordinate system whose X and Y axes are in the local horizon and Z axis points to the local Zenith is much better suited and is the industry standard. Therefore, the geocentric latitude and longitude location information is first converted into a local coordinate system, which is shown in Fig. 3. X'Y'Z' is the local coordinate system. The origin of the local coordinate system is randomly chosen to be the starting location of UAV 1. In the figure, ϕ and γ are the geocentric latitude and longitude respectively. ϕ' is the geodetic latitude [7]. Refer to [8] for a detailed description on how to convert the LLH coordinates into local coordinates.

Figures 4 - 6 show the UAV paths in 2D during a flight of 1 hour and 50 minutes. The location of the UAV is estimated from GPS, hereby referred to as GPS location. In

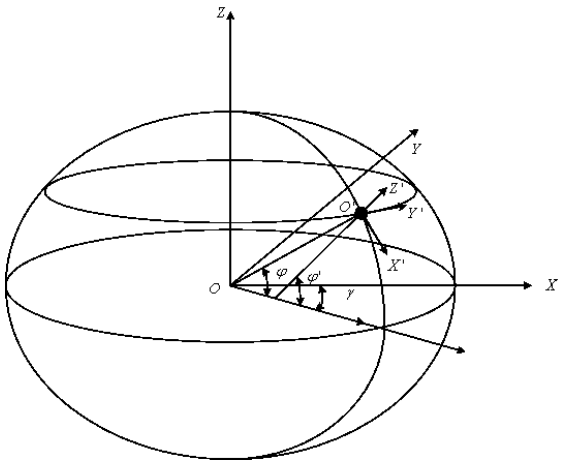

Fig. 3: Coordinate transformation. XYZ is the geocentric coordinate system and X'Y'Z' is the local coordinate system.

the local coordinate system, the z coordinates of all three UAVs vary within a range of $[-4m, 6m]$ during the flight. This small variation in the z coordinate may be attributable to the Earth's curvature and is ignored. It is also noticed that the GPS location of UAV 1 varies in a very small range. In the experiment, UAV 1 is simply a receiver installed on a stationary post. Therefore this variation in the GPS location of UAV 1 is only an artifact reflecting the GPS measurement error.

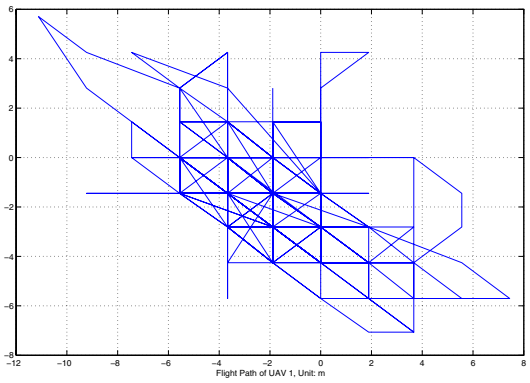

Fig. 4: Nominal flight path of UAV 1 (The UAV is actually tethered).

It is noted that for UAV 2, it may lose its GPS connection for a maximum interval of 54s. Fig. 7 shows the time interval between adjacent GPS measurements for UAV 2. This figure shows that the scenario, which motivates the research in this paper, may indeed occur in real application. Even in the benign environment of the experiment, hardware failure and satellite obscuration due to the UAV wings when it is banking can cause GPS outage.

5. Simulation

In this section, we demonstrate simulation results, which validate the proposed approach. As we shall now explain,

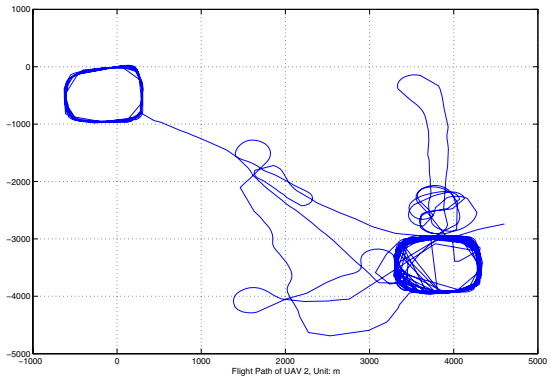

Fig. 5: Flight path of UAV 2.

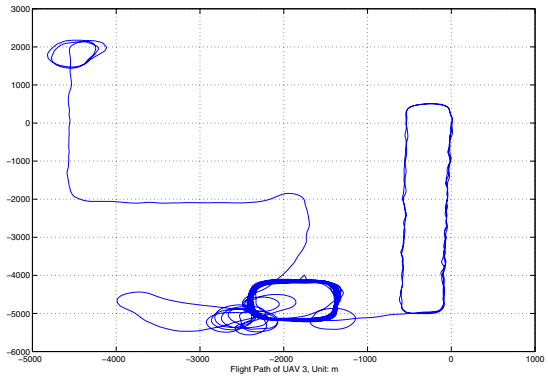

Fig. 6: Flight path of UAV 3.

these simulation results use real world data from a recent trial conducted by DSTO in Australia with three UAVs, for both simulation purposes, and the data is also used for validation.

At the present time, the UAVs are not equipped to determine inter-UAV distances; hence, as indicated in the introduction, loss of a GPS connection is likely currently to be fatal. For this reason, the real world data we use is entirely data obtained when all UAVs do actually have a GPS connection (except UAV 2 may temporarily lose its GPS connection as indicated in Fig. 7). From this data, we are able to simulate loss of a GPS connection and acquisition of inter-UAV distance measurements in the following way. A certain time series of intervals of synthetic GPS outage is postulated (as discussed in more detail below). During these intervals, inter-UAV distances are synthesized at discrete instants of time. This is done by taking the actual GPS measurements, determining the corresponding inter-UAV distance, and then adding on to the resulting value a Gaussian random variable with zero mean and standard deviation of $10m$. This is delivered to the algorithm as a (synthesized) inter-UAV distance, and the Kalman filter is run with this data.

Validation occurs by comparing the estimated UAV tracks delivered by the Kalman filter with those in the original real-

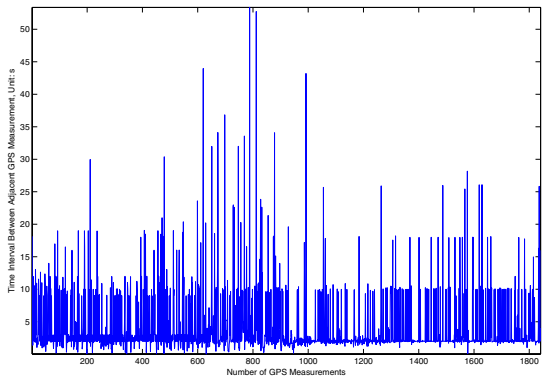

Fig. 7: Time interval between adjacent GPS measurements for UAV 2.

world data, where GPS measurements are actually available, so that actual UAV tracks are known.

In the simulations, we assume that UAV 3 never has a GPS connection and it measures its distances to UAV 1 and UAV 2 (both have known location) to estimate its location using the proposed EKF. We also assume that its initial position is sufficiently known as to avoid flip ambiguity in Fig. 1. Experimental data from DSTO showed that that UAV 1 always has a GPS connection (In fact, this is because UAV 1 is actually tethered); UAV 2 has a GPS connection most of the time but it may temporarily lose the GPS connection for up to 54s (see Fig. 7). Because when UAV 2 loses its GPS connection the inter-UAV distance between UAV 3 and UAV 2 cannot be determined, so we assume no distance measurements between UAV 2 and UAV 3 are made during the interval when UAV 2 loses its GPS connection.

As described above, synthesized distance measurements are constructed. The time interval between adjacent distance measurements between UAV 1 and UAV 3 is a sequence of independent random variables uniformly distributed in the interval $[0.875s \quad 1.125s]$; and this randomness in the time interval is intended to model the effect of inaccurate synchronization. The time interval between adjacent distance measurements between UAV 2 and UAV 3 is also a sequence of independent random variables uniformly distributed in the interval $[0.875s \quad 1.125s]$ and is independent from the first time interval sequence.

In the simulation, the first two state variables of the initial state vector are chosen to be the initial GPS location of UAV 3 and other state variables are chosen randomly. The initial value of P is chosen based on an empirical estimate as $P_{0|0} = diag\{1000 \quad 1000 \quad 0.3 \quad 0.01 \quad 1\}$. It is found that generally the choice of $P_{0|0}$ has little impact on the filter performance; however a very large deviation of $P_{0|0}$ from its true value does cause the divergence of the filter. The value of Q is chosen based on an empirical estimate as $Q = diag\{0.0003 \quad 10\}$. The choice of Q is critical for the filter performance and Q should be chosen carefully based on an in-depth understanding of the UAV dynamics. The value of R is chosen to be 100. In real applications, the value of R can be obtained via *a priori* calibration of the distance measurement equipment. The distance measurement can be obtained by a simple round trip timing mechanism.

Fig. 8 illustrates the performance of the proposed EKF. A total of $9,718$ of distance measurements to UAV 1 and UAV 2 are made during the $6,618s$ interval.

The flip ambiguity problem shown in Fig. 2 did not occur in the simulation. It is considered that in addition to distance measurements, knowledge of the UAV dynamic model is also employed in the EFK. This knowledge of UAV dynamics may help to alleviate the effect of the flip ambiguity problem.

The UAV location obtained from GPS is used as the "true location" of the UAV. The path of UAV 3 starts from the rectangular on the right side of the figure. Apparently, the estimated location has larger error on this part of the figure. As time evolves, the estimated location gradually converges to the true location, which is evidenced by much less deviation from the true location on the left side of the figure. Fig. 9 and 10 shows the variation of error in $\hat{x}$ (i.e., $\hat{x} - x$) and the variation of error in $\hat{y}$ (i.e., $\hat{y} - y$) respectively.

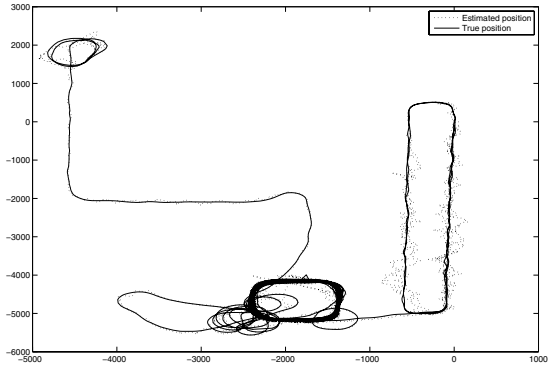

Fig. 8: An illustration of the performance of the proposed EKF.

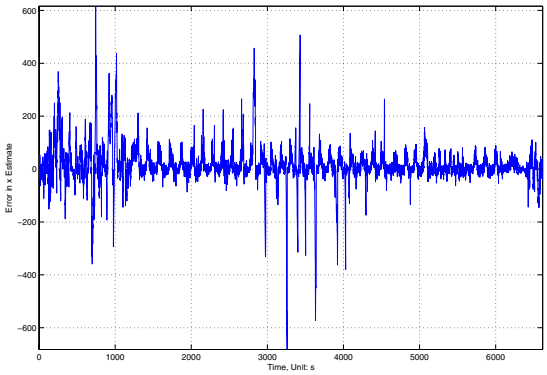

Fig. 9: Variation of error in $\hat{x}$ with Time.

The performance of the proposed EKF is measured by six metrics, i.e., the mean error of the estimated x, $E(\hat{x} - x)$, and

TABLE 1: PERFORMANCE OF THE EXTENDED KALMAN FILTER. UNIT: M.

Simulation	$E(\hat{x}-x)$	$\sigma(\hat{x}-x)$	$E(\hat{y}-y)$	$\sigma(\hat{y}-y)$	$E(\tilde{d})$	$\sigma(\tilde{d})$
1	10.5836	46.3087	-10.9167	38.1720	38.8275	48.2183
2	8.7661	45.6333	-11.7453	37.2149	37.2011	47.9382
3	10.9220	47.6161	-11.8613	38.5942	39.2297	49.7761
4	10.1834	62.1998	-12.3481	40.1211	39.0115	64.9048
5	8.7462	50.1151	-12.1389	39.2946	39.4348	52.1936
6	9.2793	45.4631	-10.8837	37.9597	38.9082	46.8867
7	9.8450	55.4412	-12.0954	39.5770	40.1785	57.1734
8	7.2842	46.6786	-12.2274	36.2379	38.4231	47.0972
9	9.2419	45.9712	-12.3221	37.8227	39.2994	47.2921
10	8.6380	52.5742	-12.3697	39.9224	40.1153	54.5532
Average	9.3490	49.8001	-11.8909	38.4917	39.0629	51.6034

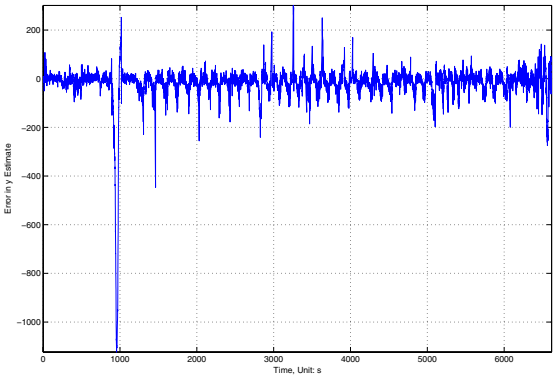

Fig. 10: Variation of error in $\hat{y}$ with Time.

the corresponding standard deviation of this error, $\sigma(\hat{x}-x)$, the mean error of the estimated y, $E(\hat{y}-y)$, and the corresponding standard deviation of the error, $\sigma(\hat{y}-y)$, the mean value of the distance between the estimated location and the true location, $E(\tilde{d})$, where

$$\tilde{d} = \sqrt{(\hat{x}-x)^2 + (\hat{y}-y)}, \tag{25}$$

and the corresponding standard deviation $\sigma(\tilde{d})$.

Table 1 shows the results from ten simulations repeated with different random seed. The last row shows the average result of the ten simulations. $9,718$ location estimates are obtained in each simulation and the first $2,000$ location estimates have been removed when calculating the performance metrics.

As shown in the Table, both the estimate of x and the estimate of y have a bias. As a reference, the value of x varies within the range of $[-5,000,\ 1,000]$ and the value of y varies within the range of $[-6,000,\ 3,000]$. These have been shown in Fig. 6. Therefore, the value of the bias is comparatively small. However, both biases have a fairly consistent trend in all ten simulations, $E(\hat{x}-x)$ is always around $9m$ and $E(\hat{y}-y)$ is always around $-11m$. Further study may be required to investigate the cause of the biases and their implications on the design of the EKF. All three values $\sigma(\hat{x}-x)$, $\sigma(\hat{y}-y)$ and $\sigma(\tilde{d})$ are around $40-50m$. There are four possible sources that may contribute to the error:

- Distance measurement error. The standard deviation of the distance measurement error is $10m$.
- Location error of GPS. This error has been shown in Fig. 4, which is around $10m$.
- The effect of an inaccurate dynamic model.
- Inaccurate knowledge of the error covariance matrix Q in Eq. 18.

6. CONCLUSION

In this paper, we proposed an EKF to estimate the location of the UAV using inter-UAV distance measurements. The proposed method may solve the practical problem that during a flight, a UAV may temporarily lose its GPS connection for a rather long time period.

We have shown that if a simple round trip timing mechanism is added to the UAVs, so that they can measure the range to other UAVs, they will be able to navigate in a GPS-denied environment as long as they are within the communication range of at least two other UAVs which have reliable GPS coordinates. The accuracy of the location estimate of the GPS-denied UAV depends on the relative position of the other UAVs but we have found that in a typical scenario in which the UAVs are separated approximately $5km$ apart and the standard deviation of the range measurement error is $10m$, the GPS-denied UAV can be localized to within $40m$ of its true location.

In our future work, we shall consider evaluating the optimality and robustness of the proposed EKF using extensive experimental data.

REFERENCES

[1] J. Z. Sasiadek and P. Hartana, "Sensor fusion for navigation of an autonomous unmanned aerial vehicle," in *IEEE International Conference on Robotics and Automation, ICRA '04*, vol. 4, 2004, pp. 4029–4034.

[2] Y. Bar-Shalom, X. R. Li, and T. Kirubarajan, *Estimation with Applications to Tracking and Navigation: Theory Algorithms and Software*. John Wiley & Sons, 2001.

[3] C. W. Martz, *Tables of the complex Fresnel integral (NASA SP-3010)*. Scientific and Technical Information Division, National Aeronautics and Space Administration, 1964.

[4] N. Ikeda *Ito's Stochastic Calculus And Probability Theory*. Springer-Verlag Telos, 1996.

[5] B. D. O. Anderson and J. B. Moore, *Optimal Filtering*. Prentice Hall, 1979.

[6] F. L. Lewis, *Optimal Estimation with An Introduction to Stochastic Control Theory*. John Wiley & Sons, 1986.

[7] A. J. Hoskinson, *Manual of geodetic astronomy;: Determination of longitude, latitude and azimuth, (United States. Coast and Geodetic Survey. Special publication)*. U.S. Govt. Print. Off, 1952.

[8] S. P. Drake, *Converting GPS coordinates $\lambda\phi h$ to local coordinates enu*. DSTO, Australia, Tech. Rep. 2000.